Atmos. Meas. Tech. Discuss., 8, 3399–3422, 2015
www.atmos-meas-tech-discuss.net/8/3399/2015/
doi:10.5194/amtd-8-3399-2015

Atmospheric Measurement Techniques Discussions
Open Access

A method to derive the Site Atmospheric State Best Estimate (SASBE) of ozone profiles from radiosonde and passive microwave data

E. Maillard Barras, A. Haefele, R. Stübi, and D. Ruffieux

Federal Office of Meteorology and Climatology, MeteoSwiss, Switzerland

Received: 21 October 2014 – Accepted: 9 March 2015 – Published: 31 March 2015

Correspondence to: E. Maillard Barras (eliane.maillard@meteoswiss.ch)

Published by Copernicus Publications on behalf of the European Geosciences Union.

Abstract

We present a method to derive the site atmospheric state best estimate (SASBE) of the ozone profile combining brightness temperature spectra around the 142 GHz absorption line of ozone measured by the microwave radiometer SOMORA and ozone profiles measured by the radiosonde (RS). The SASBE ozone profile is obtained using the radiosonde ozone profile as a priori information in an optimal estimation retrieval of the SOMORA radiometer. The resulting ozone profile ranges from ground up to 65 km altitude and makes optimal use of the available information at each altitude. The high vertical resolution of the radiosonde profile can be conserved and the uncertainty of the SASBE is well defined at each altitude.

A SASBE ozone profile dataset has been generated for Payerne, Switzerland, with a temporal resolution of 3 profiles a week for the time period ranging from 2011 to 2013. The relative difference of the SASBE ozone profiles to the AURA/MLS ozone profiles lies between −3 to 6 % over the vertical range of 20–65 km. Above 20 km, the agreement between the SASBE and AURA/MLS ozone profiles is better than the agreement between the operational SOMORA ozone data set and AURA/MLS. Below 20 km the SASBE ozone data are identical to the radiosonde measurements.

The same method has been applied to ECWMF-ERA interim ozone profiles and SOMORA data to generate a SASBE dataset with a time resolution of 4 profiles per day. These SASBE ozone profiles agree between −4 and +8 % with AURA/MLS. The improved agreement of the SASBE datasets with AURA/MLS above 20 km demonstrates the benefit of better a priori information in the retrieval of ozone from brightness temperature data.

AMTD
8, 3399–3422, 2015

1 Introduction

Since the discovery of the ozone hole over Antarctica in 1983 (Chubachi, 1985; Farman, 1985), the understanding of the mechanisms driving the variability of the stratospheric ozone layer has been one of the major area of interest in atmospheric research. Dynamical (Miyazaki, 2005) and chemical (Revell, 2012) processes are considered depending on time, location and altitude. The consideration of the entire vertical extent of the atmosphere and of the interaction between the different layers is of primary importance in understanding the stratospheric ozone variability.

At many measurement sites, ozone measurements are performed by several instruments, each of them covering a particular altitude range with different spatial or temporal resolutions. Radiosondes are measuring ozone profiles from ground up to 30–35 km (Hassler, 2013), LIDAR measurements are performed during the night up to 50 km (Pelon, 1986), and microwave radiometers (MWR) measure ozone profiles from the lower stratosphere up to the lower mesosphere with a high temporal resolution. Satellites regularly overpass the ground measurement sites and measure ozone profiles from 10 to 70 km (Hassler, 2013). Dobson and Brewer spectrometers measure the ozone total column up to more than 100 times a day depending on the meteorological situation (Scarnato, 2010). Hence, in order to obtain a continuous ozone profile ranging from the ground up to the mesosphere, the different observation methods need to be combined. This is one of the recommendations for an optimal observation strategy by GRUAN (GCOS Reference Upper Air Network) for atmospheric parameters (WMO, 2013).

Various methods for the combination of ozone profiles have been reported in the literature in the perspective of a temporal (DeLand, 2012) or spatial (Bodeker, 2012) merging of datasets. In particular, when complementary but overlapping vertical profiles shall be merged, the data have to be represented on the same vertical grid in the overlap region. Generally, the coarser grid is chosen and the high resolution data are downscaled to the lower resolution. This can be achieved by using the Curtis–

AMTD
8, 3399–3422, 2015

Godson equation (Goody, 1989) which conserves the column density in the profile to be downscaled. If an averaging kernel is provided along with the low resolution data, the high resolution data can be convoluted with this averaging kernel (Tsou, 1995; Calisesi, 2005). A third method to downscale the high resolution data consists of applying a Gaussian filter centered around the levels of the coarse grid on the high resolution data as it has been done for the "Binary Database of Profiles" of Hassler et al. to combine ozone sonde and satellite vertical profiles (Hassler, 2008). Finally, Livesey et al. (2011) suggest to compute the inverse of matrix **A** which describes the linear interpolation from the coarse to the high resolution grid and to apply $\mathbf{A}^{-1}$ to the high resolution data. For instruments with similar vertical resolution or once the vertical resolution has been adjusted using one of the methods explained above, a linear interpolation in the logarithm-pressure vertical coordinate can be used in the overlap region to merge the profiles (Sofieva, 2014). These merging methods do not preserve the original vertical resolution of the profiles involved in the combination, the vertical resolution of the combined profiles being either one of the original resolutions or a new common resolution. Alternatively, data can also be combined on the level of the raw data. Timofeyev et al. (2013) have proposed to combine Fourier transform infrared radiometer (FTIR) and MWR spectral data by retrieving a single ozone profile simultaneously from both spectral measurements or by sequential retrievals using the profile and the covariance matrix of the first retrieval step (FTIR) as an a priori information for the second retrieval step (MWR). This method allows to choose the vertical grid freely or to optimize it given the degrees of freedom of the retrieval.

At the measurement site of MeteoSwiss in Payerne, ozone measurements are performed by radiosondes (Stübi, 2008) since 1968 and by microwave radiometry since 2000 (Calisesi, 2000). Here, we propose to combine the simultaneous radiosonde and microwave radiometer measurements to obtain the SASBE of the vertical ozone distribution above the site. The two measurements are combined by using the radiosonde ozone profile as a priori information in the optimal estimation retrieval of the microwave radiometer. This merging method is new in the sense that the original vertical resolutions of the radiosonde ozone profiles and of the microwave ozone profiles are preserved in the SASBE ozone profiles and that the uncertainty is well characterized at each altitude level.

The paper is organized as follows: Sect. 2 deals with the description of the instruments, and of the measured and simulated datasets used in the study. A detailed description of the merging method and a characterization of the retrieved profiles are given in Sects. 3 and 4. In Sect. 5, the SASBE ozone profiles are compared to simultaneous satellite ozone profiles measured by AURA/MLS. The agreement of SASBE ozone profiles, using either RS or ECMWF ozone profiles, and of SOMORA ozone profiles with MLS ozone profile are finally discussed.

2 Instruments and models

2.1 Stratospheric Ozone Monitoring Radiometer SOMORA

Developed in 2000 by the University of Bern (Calisesi, 2000), the SOMORA is a total power microwave radiometer measuring the thermal emission line of ozone at 142.175 GHz. The electromagnetic radiation is measured under an antenna elevation angle of 39° and the brightness temperatures range from 80 to 260 K. The SOMORA is calibrated using a hot load heated and stabilized at 300 K and a cold load at 77 K cooled with liquid nitrogen. A rotating planar mirror is used as a switch between the radiation sources. A Martin–Puplett interferometer (sideband filter) picks out the frequency band around 142 GHz. Outgoing from the front-end part (quasi optics), the signal is amplified and down-converted in frequency to 7.1 GHz by means of a constant-frequency signal (mixer). The signal is further down-converted in two steps (intermediate step at 1.5 GHz/1 GHz) to the baseband (0–1 GHz). The spectral distribution, i.e. voltage as function of channel or frequency is measured since 10/2010 by an Acquiris Fast–Fourier–Transform spectrometer (FFTS) with 16 384 channels distributed over 1 GHz bandwidth. Before, two acousto-optical spectrometers (AOS) have been used for spectral detection (Calisesi, 2000). This study has been performed using spectra measured after the FFTS upgrade of the instrument.

After 30 min integration time, an ozone volume mixing ratio (VMR) profile is retrieved by optimal estimation using ARTS/Qpack, which is a general environment for the radiative transfer simulation (forward model) (Buehler, 2005) and the optimal estimation method (OEM) profile retrieval of Rodgers (Eriksson, 2005). The vertical resolution of the ozone profiles is 8–10 km from 20 to 40 km, increasing to 15–20 km at 60 km.

The measured spectrum $\boldsymbol{y}$ is a function $F(\boldsymbol{x},\boldsymbol{b})$ of the vertical distribution of ozone $\boldsymbol{x}$ and forward model parameters $\boldsymbol{b}$ (atmospheric temperature, spectroscopic data, measurement geometry, ...). The OEM solution $\hat{\boldsymbol{x}}$ to the inverse problem minimizes the cost function χ^2 derived from the Bayesian theory:

$$\chi^2 = [\boldsymbol{y} - F(\boldsymbol{x},\boldsymbol{b})]^T \mathbf{S}_y^{-1} [\boldsymbol{y} - F(\boldsymbol{x},\boldsymbol{b})] + \left[\boldsymbol{x} - \boldsymbol{x}_\mathrm{a}\right]^T \mathbf{S}_\mathrm{a}^{-1} \left[\boldsymbol{x} - \boldsymbol{x}_\mathrm{a}\right] \quad (1)$$

where $\boldsymbol{y}$ is the measured spectrum, $F(\boldsymbol{x},\boldsymbol{b})$ the calculated spectrum corresponding to the ozone profile $\boldsymbol{x}$ and model parameters $\boldsymbol{b}$, $\boldsymbol{x}$ the true ozone profile, $\mathbf{S}_y$ the error covariance matrix of the measured spectrum, $\boldsymbol{x}_\mathrm{a}$ the a priori ozone profile and $\mathbf{S}_\mathrm{a}$ the error covariance matrix of the a priori ozone profile.

The optimal estimation method takes into account the uncertainties of the measured spectrum specified in $\mathbf{S}_y$ and uses a priori information specified by $\boldsymbol{x}_\mathrm{a}$ and $\mathbf{S}_\mathrm{a}$ to constrain the solution $\hat{\boldsymbol{x}}$ to statistically probable profiles. In the operational data processing of SOMORA two different a priori ozone profiles are used, one for summer and one for winter. These a priori profiles are derived from the two standard model ozone profiles described in (Keating, 1990) combining 5 satellite ozone data sets (among them SAGE and SBUV). The diagonal elements of the a priori covariance matrix are given by the variance of a climatology of Payerne radiosondes below 25 km and of a climatology of MWR ozone profiles above 25 km (climatology of the microwave radiometer GROMOS, another NDACC instrument based in Bern, Switzerland, Calisesi, 2000). The off-diagonal elements are parameterized with an exponentially decaying correlation function using a correlation length of 3 km. The retrieval $\hat{\boldsymbol{x}}$ is characterized by the

AMTD
8, 3399–3422, 2015

averaging kernel (AVK) matrix describing the changes in the retrieved profile, $\partial\hat{\boldsymbol{x}}$, as a function of changes in the true profile, $\partial\boldsymbol{x}$:

$$\mathbf{AVK} = \frac{\partial\hat{\boldsymbol{x}}}{\partial\boldsymbol{y}}\frac{\partial\boldsymbol{y}}{\partial\boldsymbol{x}} \tag{2}$$

The AVK shows the sensitivity of the retrieved profile to the changes of the true profile. For an ideal observing system, the **AVK** is equal to the unity matrix. For a real instrument, the width of the AVKs is a measure of the resolution of the system (Rodgers, 1990). The area of the AVKs is indicating the measurement contribution to the retrieved profile. The total uncertainty of the retrieved profile consists of the observation and the smoothing error. The smoothing error is the error contribution due to the smoothing of the true state by the AVK. The observation error is to the greatest extent due to the thermal noise in the spectral data, and to minor extent due to errors in the Temperature profile and the antenna elevation angle error, which are part of the forward model parameters $\boldsymbol{b}$. The observation error is less than 3 % between 20 and 40 km, but increases to 7 % in the upper stratosphere.

The total error (sum of observation error and smoothing error) is less than 10 % between 20 and 40 km, 15 % at 50 km, and greater than 25 % below 15 and above 60 km.

SOMORA has been extensively used in comparisons with AURA/MLS and SAGE (Hocke, 2007), ENVISAT (Hocke, 2006), LIDAR (Calisesi, 2003a), and radiosonde (Calisesi, 2003b). SOMORA belongs to the Network for the Detection of Atmospheric Composition Change (NDACC).

2.2 Ozone radiosonde

Ozone sondes are launched from Payerne since 1968 (Stübi, 2008). The ozone sonde consists of an electrochemical cell where the reaction of ozone with potassium iodide in aqueous solution is used to measure continuously the ozone concentration. An electrical current is generated which is proportional to the rate at which ozone enters the cell.

AMTD
8, 3399–3422, 2015

The ozone concentration is determined from the electric current measurement considering the airflow rate, the air pressure, and the pump temperature. Since September 2002, the electrochemical concentration cell (ECC) with 0.5 % KI concentration is the operational ozone sensor for Payerne.

Ozone is measured in the altitude range of 0 to 30–35 km every Monday, Wednesday and Friday. The vertical resolution is 150 m and the uncertainty of the ozone measurement is of the order of 5–10 % depending on the altitude (Stübi, 2008; Dabberdt, 2003).

Payerne ozone sonde profiles are submitted to WOUDC and NDACC on an operational basis, and are extensively used in satellite validation programs (Meijer, 2004) and ozone assessments (Douglass, 2011).

2.3 ECMWF ERA-Interim model

Six hourly ozone profiles from ERA-Interim are used in this study. The ERA-Interim reanalysis is produced with a sequential data assimilation scheme described in Dee et al. (2011). Ozone is analysed simultaneously with the other model state variables in the 4D-Var analysis. At a given point of the atmosphere, the continuity equation for ozone is given as a linear relaxation towards a photochemical equilibrium for the ozone mixing ratio, the temperature, and the ozone column. The photochemical loss term is a function of the equivalent chlorine content for the actual year. A large variety of satellite observations are assimilated: MIPAS, SCIAMACHY, TOMS, GOME, MLS, OMI (Dragani, 2010). The ozone sonde data are not assimilated in ERA-Interim but comparisons are described by Dragani et al. (2010). At midlatitudes in the Northern Hemisphere, the agreement between sondes and ERA-Interim is within 5 % in the troposphere. The seasonal variability is well captured for total ozone and temporal occurrence with an agreement of 10 % in the stratosphere. However, the ozone peak is underestimated by ERA-Interim in summer periods, with relative biases of about 20 % (Dragani, 2010). ERA-Interim ozone profiles are given on 60 pressure levels with the top of the atmosphere at 0.1 hPa.

AMTD
8, 3399–3422, 2015

3 Method

The SASBE of ozone is computed using the radiosonde measurement as a priori information in the optimal estimation retrieval of SOMORA, which is described in Sect. 2.1. The retrieval grid, i.e. the grid of the resulting SASBE ozone profile, is equal to the standard grid of the radiosonde profile up to 25 km with a grid spacing of 500 m. Above 25 km, the standard SOMORA retrieval grid is used with a grid spacing of 2500 m. The a priori profile is identical to the radiosonde ozone measurement below 23 km. Above 35 km the standard SOMORA a priori profile is chosen as explained in Sect. 2.1. In order to avoid discontinuities in the a priori profile $\boldsymbol{x}_a$, a weighting function f increasing linearly from 0 to 1 between 23 and 35 km is applied to the standard a priori $\boldsymbol{x}_{SOM}$, which has been interpolated to the high resolution grid, and the radiosonde profile $\boldsymbol{x}_{RS}$ (see Fig. 1):

$$\boldsymbol{x}_a = f\,\boldsymbol{x}_{SOM} + (1-f)\,\boldsymbol{x}_{RS} \tag{3}$$

Since the a priori profile below 23 km comes from the radiosonde measurement, the diagonal elements of the a priori covariance matrix $\mathbf{S}_a$ are populated with the square of measurement uncertainties of the radiosonde measurement as specified in Sect. 2.2. Above 23 km the diagonal elements are identical to the a priori covariance matrix of the standard SOMORA retrieval as described in Sect. 2.1.

The off-diagonal elements are parameterized with an exponentially decaying correlation function using a correlation length of 150 m below 25 km which corresponds to the vertical resolution of the RS ozone profile.

The SASBE retrieval provides an ozone profile from the surface up to 65 km that is based on measurements. Whether the information comes from the radiosonde or the microwave measurement is determined by the confidence in the measurement and the a priori profile, i.e. by $\mathbf{S}_y$ and $\mathbf{S}_a$. Visual inspection of Fig. 2b shows that the information in the SASBE comes to the greatest extent from the a priori profile below 25 km and from the microwave measurement above, as expected. Section 4 will deal with the detailed explanation of the characterization of the SASBE profile based on Fig. 2.

AMTD
8, 3399–3422, 2015

A SASBE is also generated using ECMWF-ERA interim. In that case the ECMWF-ERA interim ozone profiles are processed in the same way as the radiosonde but we refer to "SASBE using ECMWF". The diagonal elements of the a priori covariance matrix below 23 km are the square of the model uncertainties estimated through the comparison of ECMWF-ERA interim data with ECC radiosonde profiles (see Sect. 2.3). The off-diagonal elements are kept the same as in the standard SOMORA retrieval.

4 Characterization of the SASBE ozone profile

The SASBE ozone profile is characterized by the AVK functions and by the uncertainties shown in Figs. 2 and 3, respectively.

The AVKs are plotted in Fig. 2a for the SOMORA retrieval and in Fig. 2b and c for the SASBE retrieval. In the case of SOMORA retrieval, the AVKs vanish below approximately 15 km indicating that the measurement does not contain any information about ozone below this altitude. In the case of the SASBE retrieval, it can be seen that the AVKs tend to zero already at 25 km which is due to the fact that a much higher confidence in the a priori profile has been specified (Fig. 2b). Similar smoothing of the true state above 30 km are shown for both retrievals by the width of the AVK functions. However, to give a complete characterization of the SASBE retrieval with the AVKs, the a priori profile below 25 km must be considered as a measurement. Therefore any variation in the true atmosphere is captured in the a priori profile and seen in the SASBE profile. The complete **AVK** as shown in Fig. 2c has been calculated with a perturbation approach: a true ozone profile has been assumed from which both the radiosonde and the microwave radiometer measurements have been calculated. The calculated measurements have been processed by the SASBE algorithm providing the retrieval for the unperturbed profile. Then the true profile has been perturbed with 1 ppm additional ozone at layer i. The measurements have been simulated from the perturbed state and processed by the SASBE algorithm providing the retrieval for the perturbed state. Note that for levels below 23 km the a priori profile is also perturbed, since it

AMTD
8, 3399–3422, 2015

is taken from the radiosonde measurement in the SASBE algorithm. The difference between the retrieval of the perturbed state and the unperturbed state divided by the norm of the perturbation yields the averaging kernel function for level i. The procedure is repeated for all levels to form the averaging kernel matrix.

The complete **AVK** show clearly the very high sensitivity and vertical resolution in the altitude range where the in situ radiosonde measurement is available, similar to an ideal measurement system.

The uncertainties of the SOMORA and the SASBE retrievals are shown in Fig. 3. It is in the nature of the optimal estimation method that the error become equal to the a priori errors in the altitude ranges where the measurement contribution is small. Therefore, the errors increase below 20 and above 60 km to the a priori uncertainties. In the case of the SOMORA retrieval, the error below 20 km increases to 35 % due to the large a priori uncertainty while the error of the SASBE retrieval remains small at 6 % below 20 km reflecting the low a priori error. The error is in both cases around 10 % at 40 km.

An example of a SOMORA and SASBE retrieval is shown in Fig. 4. The SASBE shows a very good correspondence to the RS ozone profile in dashed red. A very good correspondence is also shown between the ECMWF profile in dashed blue and the SASBE using ECMWF ozone profile in solid blue.

The sampling rate of the SASBE ozone profile dataset is 3 times a week for the combination of RS and MWR data and 4 times a day for the combination of ECMWF model and MWR ozone profiles. The ozone profile time series over Payerne are available in a special dataset (shown in nbar for 2 monthes in Fig. 5) composed by MWR ozone profiles in the range of 20 to 65 km each 30 min (in black), SASBE ozone profiles 3 times a week (in red) in the range of ground up to 65 km and SASBE using ECMWF 4 times a day (in dashed blue) in the range of ground up to 65 km.

AMTD
8, 3399–3422, 2015

5 Validation by comparison to AURA/MLS and Payerne RS

Payerne SASBE and SASBE using ECMWF ozone profiles from 2011 to 2013 have been compared to simultaneous MLS and radiosonde measurements. The following time and spatial coincidence conditions have been chosen in order to ensure reasonable overpass statistics while avoiding sampling issues. The time coincidence condition is ±4 h and the spatial coincidence condition is ±2.5° in latitude and ±5° in longitude. Payerne RS time coincidence condition is ±1 h.

Above 25 km, MLS ozone profile have been downscaled to the vertical resolution of SOMORA resp. SASBE using AVK smoothing (Tsou, 1995) as follows:

$$\mathbf{X}_{\text{sat, low}} = \mathbf{X}_{\text{apriori, SOMORA resp. SASBE}} + \mathbf{A}_{\text{SOMORA resp. SASBE}} (\mathbf{X}_{\text{sat, high}} - \mathbf{X}_{\text{apriori, SOMORA resp. SASBE}}) \quad (4)$$

$$\mathbf{X}_{\text{RS, low}} = \mathbf{X}_{\text{apriori, SOMORA resp. SASBE}} + \mathbf{A}_{\text{SOMORA resp. SASBE}} (\mathbf{X}_{\text{RS, high}} - \mathbf{X}_{\text{apriori, SOMORA resp. SASBE}}) \quad (5)$$

$\mathbf{X}_{\text{apriori, SOMORA resp. SASBE}}$ is the a priori profile of the standard SOMORA and the SASBE retrieval, respectively, and $\mathbf{A}_{\text{SOMORA resp. SASBE}}$ is the averaging kernel matrix of the corresponding retrieval. $\mathbf{X}_{\text{sat, low}}$ resp. $\mathbf{X}_{\text{RS, low}}$ is the downscaled profile of the satellite and RS measurement, respectively, adjusted to the vertical resolution of the SASBE.

The arithmetic averages of the relative differences of SOMORA resp. SASBE to MLS and RS are shown in Fig. 6a and b. The relative difference between the RS ozone profiles and the SASBE (using RS) profiles is smaller than 6 % below 20 km with no systematic bias as expected. The SASBE using ECMWF profiles show a difference with RS profiles as high as 35 % at 15 km. This is in accordance with the relative difference between ECWMF ERA Interim and RS ozone profiles as reported in Dragani et al. (2010).

SOMORA ozone profiles show a good correspondence to MLS with a difference between +6 and +10 % over the whole common measurement range. SASBE ozone profiles agree within 6 % with MLS/AURA satellite ozone profiles which is a slight improvement compared to standard SOMORA ozone profiles. This improvement is related to the fact that smaller a priori errors below 25 km are lowering the cost corresponding to the state vector and therefore influencing the retrieval stability well over the RS altitude range. The SASBE using ECMWF agrees within 8 % with MLS which is also slightly better than the standard SOMORA retrieval. The SD of the relative differences is between 15 and 20 % for standard SOMORA and SASBE. Comparisons below 25 km show that the SASBE is unbiased compared to the radiosonde and that the proposed method does not have any degrading effect on the lower part of the profile.

6 Conclusions

Ozone profiles measured simultaneously by microwave radiometry and radio sounding over Payerne have been combined in one single ozone profile conserving maximum vertical resolution of both measurements. In the presented approach, the radiosonde ozone profile has been used as the a priori information in the optimal estimation retrieval of the SOMORA radiometer. The a priori covariance matrix has been adjusted representing the measurement uncertainty of the radiosonde in the corresponding altitude range, i.e. below 25 km. The resulting profile, called SASBE, makes an optimal use of the available information at each altitude of the range and is fully characterized in terms of uncertainty and vertical resolution. An extended **AVK** has been calculated representing the total measurement process including the radiosonde. It reveals that the SASBE is sensitive to atmospheric variations at altitudes from the ground up to approximately 65 km. The uncertainty of the SASBE is 5 % up to 30 km and increases nearly linearly above to 25 % at 65 km.

A new 3 year dataset of SASBE and SASBE using ECMWF ozone profiles has been generated with a temporal sampling of 3/week and 4/day, respectively. The vertical range of the profiles composing the dataset goes from the ground to 65 km for the

SASBE ozone profiles compared to a range from 20 to 65 km in the case of the standard SOMORA retrieval.

The SASBE and SASBE using ECMWF data sets have been validated against Aura/MLS ozone profiles. The comparison revealed an improved agreement with Aura/MLS in the altitude range from 25 to 65 km for both data sets compared to the standard SOMORA retrieval. This improvement is clearly attributed to the better a priori information below 25 km and is remarkable since the improvement is seen at higher altitudes.

The SASBE dataset over Payerne is available for validation of satellite and other remote sensing instrument ranging from ground to 65 km height with a temporal resolution of 3 times a week for SASBE (using RS) and of 6 h for SASBE using ECMWF.

The presented approach to combine measurements is equivalent to 1-D variational data assimilation. It can be considered as a general framework for data fusion and provides a single atmospheric state that is consistent with an arbitrary number of observations allowing for a detailed characterization of the result in terms of uncertainty and resolution.

Acknowledgements. This work has been funded by MeteoSwiss within the Swiss Global Atmospheric Watch (GAW) program of the World Meteorological Organization.

References

Bodeker, G. E., Hassler, B., Young, P. J., and Portmann, R. W.: A vertically resolved, global, gap-free ozone database for assessing or constraining global climate model simulations, Earth Syst. Sci. Data, 5, 31–43, doi:10.5194/essd-5-31-2013, 2013.

Buehler, S. A., Eriksson, P., Kuhn, T., von Engeln, A., and Verdes, C.: ARTS, the Atmospheric Radiative Transfer Simulator, J. Quant. Spectrosc. Ra., 91, 65–93, doi:10.1016/j.jqsrt.2004.05.051, 2005.

Calisesi, Y.: Monitoring of Stratospheric and Mesospheric Ozone with a Ground-Based Microwave Radiometer: Data Retrieval, Analysis, and Applications, Ph.D. thesis, Philosophisch-

Naturwissenschaftliche Fakultät, Universität Bern, Bern, Switzerland, 77 pp., available at: http://www.iap.unibe.ch/publications (last access: 20 March 2015), 2000.
Calisesi, Y., Ruffieux, D., Kämpfer N., and Viatte, P.: The Stratospheric Ozone Monitoring Radiometer SOMORA: first validation results, in: Proceedings of the Sixth European Symposium on Stratospheric Ozone, Göteborg, Sweden, 2–6 September 2002, 92–95, 2003a.
Calisesi, Y., Stuebi, R., Kämpfer, N., and Viatte, P.: Investigation of systematic uncertainties in Brewer–Mast ozone soundings using observations from a ground-based microwave radiometer, J. Atmos. Ocean. Tech., 20, 1543–1551, 2003b.
Calisesi, Y., Soebijanta, V. T., and van Oss, R. O.: Regridding of remote soundings: formulation and application to ozone profile comparison, J. Geophys. Res., 110, D23306, doi:10.1029/2005JD006122, 2005.
Chubachi, S.: A special ozone observation at Syowa station, Antarctica from February 1982 to January 1983, in: Atmospheric Ozone, edited by: Zerefos, C. and Ghazi, A., Springer Netherlands, 6099, 285–289, doi:10.1007/978-94-009-5313-0_58, 1985.
Dabberdt, W. F. and Shellhorn, R.: Radiosondes, edited by: Shankar, M., available at: http://radiosondemuseum.org/wp-content/uploads/2012/10/RadiosondeArticle.pdf (last access: 20 March 2015), 2003.
Dee, D. P., Uppala, S. M., Simmons, A. J., Berrisford, P., Poli, P., Kobayashi, S., Andrae, U., Balmaseda, M. A., Balsamo, G., Bauer, P., Bechtold, P., Beljaars, A. C. M., van de Berg, L., Bidlot, J., Bormann, N., Delsol, C., Dragani, R., Fuentes, M., Geer, A. J., Haimberger, L., Healy, S. B., Hersbach, H., Holm, E. V., Isaksen, L., Kallberg, P., Köhler, M., Matricardi, M., McNally, A. P., Monge-Sanz, B. M., Morcrette, J., Park, B., Peubey, C., de Rosnay, P., Tavolato, C., Thépaut, J., Vitart, F.: The ERA-Interim reanalysis: configuration and performance of the data assimilation system, Q. J. Roy. Meteor. Soc., 137, 553–597, doi:10.1002/qj.828, 2011.
DeLand, M. T., Taylor, S. L., Huang, L. K., and Fisher, B. L.: Calibration of the SBUV version 8.6 ozone data product, Atmos. Meas. Tech., 5, 2951–2967, doi:10.5194/amt-5-2951-2012, 2012.
Douglass, A., Fioletov, V., (Coordinating Lead Authors), Godin-Beekmann, S., Müller, R., Stolarski, R. S., and Webb, A.: Stratospheric ozone and surface ultraviolet radiation, in: Scientific Assessment of Ozone Depletion: 2010, Global Ozone Research and Monitoring Project–Report No. 52, World Meteorological Organization, Geneva, Switzerland, 2.15, 2011.

AMTD
8, 3399–3422, 2015

A method to derive the SASBE of ozone profiles

E. Maillard Barras et al.

Dragani, R.: On the quality of the ERA-Interim ozone reanalyses, Part I: Comparisons with in situ measurements, ERA Report Series, No. 2, ECMWF, Reading, UK, 2010.
Eriksson, P., Jimenez, C., and Buehler, S. A.: Qpack, a general tool for instrument simulation and retrieval work, J. Quant. Spectrosc. Ra., 91, 47–64, doi:10.1016/j.jqsrt.2004.05.050, 2005.
Farman, J. C., Gardiner, B. G., and Shanklin, J. D.: Large losses of total ozone in Antarctica reveal seasonal ClO_x/NO_x interaction, Nature, 315, 207–210, doi:10.1038/315207a0, 1985.
Goody, R. M. and Jung, Y. L.: Atmospheric Radiation: Theoretical Basis, 2nd edn., Oxford Univ. Press, New York, 519 pp., 1989.
Hassler, B., Bodeker, G. E., and Dameris, M.: Technical Note: A new global database of trace gases and aerosols from multiple sources of high vertical resolution measurements, Atmos. Chem. Phys., 8, 5403–5421, doi:10.5194/acp-8-5403-2008, 2008.
Hassler, B., Petropavlovskikh, I., Staehelin, J., August, T., Bhartia, P. K., Clerbaux, C., Degenstein, D., Mazière, M. De, Dinelli, B. M., Dudhia, A., Dufour, G., Frith, S. M., Froidevaux, L., Godin-Beekmann, S., Granville, J., Harris, N. R. P., Hoppel, K., Hubert, D., Kasai, Y., Kurylo, M. J., Kyrölä, E., Lambert, J.-C., Levelt, P. F., McElroy, C. T., McPeters, R. D., Munro, R., Nakajima, H., Parrish, A., Raspollini, P., Remsberg, E. E., Rosenlof, K. H., Rozanov, A., Sano, T., Sasano, Y., Shiotani, M., Smit, H. G. J., Stiller, G., Tamminen, J., Tarasick, D. W., Urban, J., van der A, R. J., Veefkind, J. P., Vigouroux, C., von Clarmann, T., von Savigny, C., Walker, K. A., Weber, M., Wild, J., and Zawodny, J. M.: Past changes in the vertical distribution of ozone – Part 1: Measurement techniques, uncertainties and availability, Atmos. Meas. Tech., 7, 1395–1427, doi:10.5194/amt-7-1395-2014, 2014.
Hocke, K., Haefele, A., Le Drian, C., Kaempfer, N., Ruffieux, D., von Clarmann, T., Milz, M., Steck, T., Froidevaux, L., Pumphrey, H. C., Jimenez, C., Walker, K. A., Bernath, P., Timofeyev, Y. M., and Polyakov, A. V.: Cross-validation of recent satellite and ground-based measurements of ozone and water vapor in the middle atmosphere, in: ESA Atmospheric Science Conference 2006, Frascati, Italy, 8–12 May 2006.
Hocke, K., Kämpfer, N., Ruffieux, D., Froidevaux, L., Parrish, A., Boyd, I., von Clarmann, T., Steck, T., Timofeyev, Y. M., Polyakov, A. V., and Kyrölä, E.: Comparison and synergy of stratospheric ozone measurements by satellite limb sounders and the ground-based microwave radiometer SOMORA, Atmos. Chem. Phys., 7, 4117–4131, doi:10.5194/acp-7-4117-2007, 2007.

Keating, G. M., Pitts, M. C., and Young, D. F.: Ozone reference models for the middle atmosphere, Adv. Space Res., 10, 12-317–12-355, 1990.
Livesey, N. J., Read, W. G., Froidevaux, L., Lambert, A., Manney, G. L., Pumphrey, H. C., Santee, M. L., Schwartz, M. J., Wang, S., Cofeld, R. E., Cuddy, D. T., Fuller, R. A., Jarnot, R. F., Jiang, J. H., Knosp, B. W., Stek, P. C., Wagner, P. A., and Wu, D. L.: Version 3.3 Level 2 data quality and description document, California Institute of Technology, Pasadena, California, available at: http://mls.jpl.nasa.gov/data/v3-3_data_quality_document.pdf (last access: 20 March 2015), 2011.
Meijer, Y. J., Swart, D. P. J., Koelemeijer, R., Allaart, M., Andersen, S., Bodeker, G., Boyd I., Braathen, G., Calisesi, Y., Claude, H., Dorokhov, V., von der Gathen, P., Gil, M., Godin-Beekmann, S., Goutail, F., Hansen, G., Karpetchko, A., Keckhut, P., Kelder, H., Kois, B., Koopman, R., Lambert, J., Leblanc, T., McDermid, I. S., Pal, S., Raffalski, U., Schets, H., Stubi, R., Suortti, T., Visconti, G., and Yela, M.: Pole-to-pole validation of ENVISAT GOMOS ozone profiles using data from ground-based and balloon-sonde measurements, J. Geophys. Res., 109, 2156–2202, doi:10.1029/2004JD004834, 2004.
Miyazaki, K., Iwasaki, T., Shibata, K., and Deushi, M.: Roles of transport in the seasonal variation of the total ozone amount, J. Geophys. Res., 110, D18309, doi:10.1029/2005JD005900, 2005.
Pelon, J., Godin, S., and Mégie, G.: Upper stratospheric (30–50 km) lidar observations of the ozone vertical distribution, J. Geophys. Res., 91, 8667–8671, doi:10.1029/JD091iD08p08667, 1986.
Revell, L. E., Bodeker, G. E., Huck, P. E., Williamson, B. E., and Rozanov, E.: The sensitivity of stratospheric ozone changes through the 21st century to N_2O and CH_4, Atmos. Chem. Phys., 12, 11309–11317, doi:10.5194/acp-12-11309-2012, 2012.
Rodgers, D. C.: Characterisation and error analysis of profiles retrieved from remote sensing measurements, J. Geophys. Res., 95, 5587–5595, 1990.
Stübi, R., Levrat, G., Hoegger, B., Viatte, P., Staehelin, J., and Schmidlin, F. J.: In-flight comparison of Brewer–Mast and electrochemical concentration cell ozonesondes, J. Geophys. Res., 113, D13302, doi:10.1029/2007JD009091, 2008.
Sofieva, V. F., Tamminen, J., Kyrölä, E., Mielonen, T., Veefkind, P., Hassler, B., and Bodeker, G.E.: A novel tropopause-related climatology of ozone profiles, Atmos. Chem. Phys., 14, 283–299, doi:10.5194/acp-14-283-2014, 2014.

Scarnato, B., Staehelin, J., Stübi, R., and Schill, H.: Long term total ozone observations at Arosa (Switzerland) with Dobson and Brewer instruments (1988–2007), J. Geophys. Res., 115, D13306, doi:10.1029/2009JD011908, 2010.
Timofeyev, Y., Kostsov, V., and Virolainen, Y.: Synergetic ground-based methods for remote measurements of ozone vertical profiles, AIP Conf. Proc., 1531, 380, doi:10.1063/1.4804786, 2013.
Tsou, J. J., Connor, B. J., Parrish, A., McDermid, I. S., and Chu, W. P.: Ground-based microwave monitoring of middle atmosphere ozone: comparison to lidar and Stratospheric and Gas Experiment II satellite observations, J. Geophys. Res., 100, 3005–3016, 1995.
WMO: WMO Integrated Global Observing System (WIGOS), Global Climate Observing System (GCOS), The GCOS Reference Upper Air Network (GRUAN) Guide, March 2013, Technical Report No. 201303, GCOS171, 68–70, available at: http://www.wmo.int/pages/prog/gcos/Publications/gcos-171.pdf (last access: 20 March 2015), 2013.

AMTD
8, 3399–3422, 2015

A method to derive the SASBE of ozone profiles

E. Maillard Barras et al.

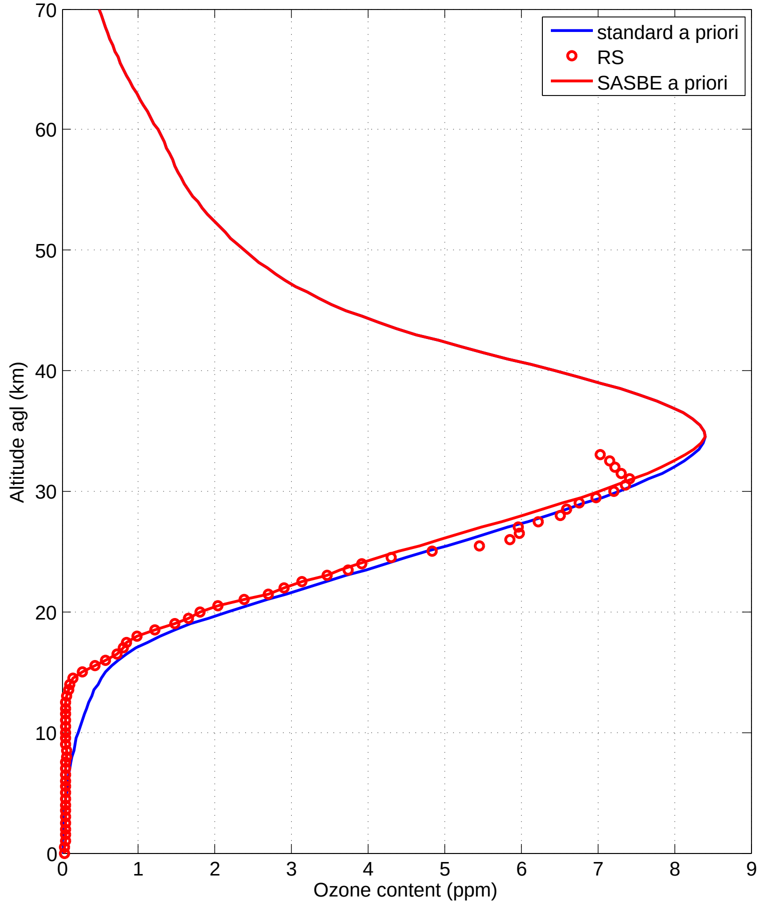

Figure 1. A priori of SASBE ozone profile retrieval in ppm in function of altitude. Combination of the summer standard a priori ozone profile in blue and of one RS ozone profile (red circles).

AMTD
8, 3399–3422, 2015

A method to derive the SASBE of ozone profiles

E. Maillard Barras et al.

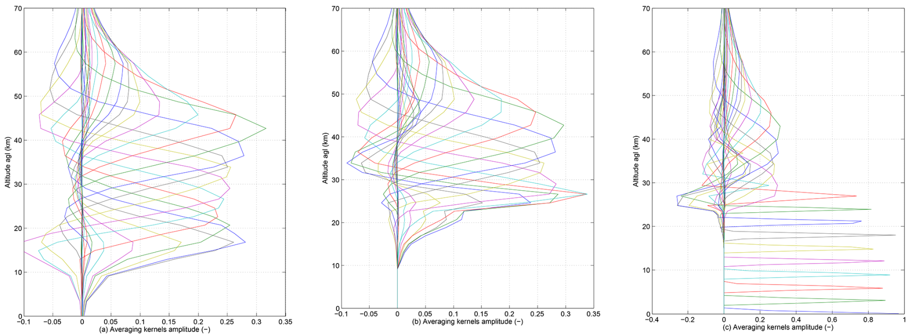

Figure 2. Averaging kernels in fraction of profile for SOMORA ozone profile of 7 October 2011, 12:00 UTC **(a)** and the corresponding SASBE ozone profile **(b)**. **(c)** SASBE averaging kernels by simulation of perturbations considering the a priori profile below 25 km as part of the measurement.

AMTD
8, 3399–3422, 2015
A method to derive the SASBE of ozone profiles
E. Maillard Barras et al.

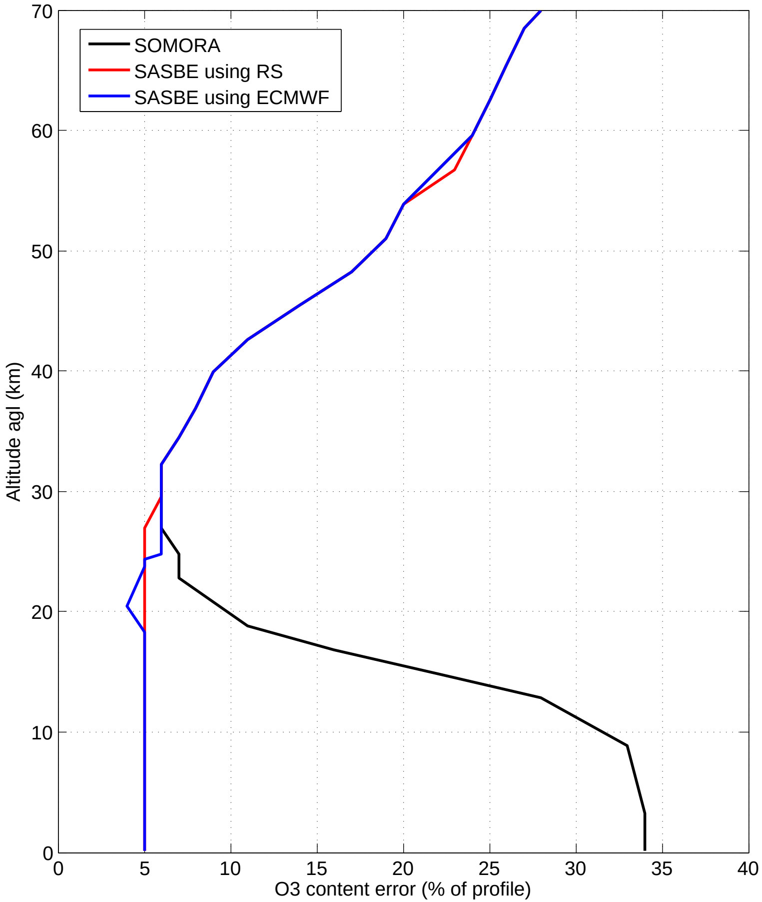

Figure 3. Profiles of the error of the SOMORA (black) and the SASBE using RS resp ECMWF ozone profiles (red resp.blue), Payerne, 24 January 2011, 12:00 UTC.

AMTD

8, 3399–3422, 2015

A method to derive the SASBE of ozone profiles

E. Maillard Barras et al.

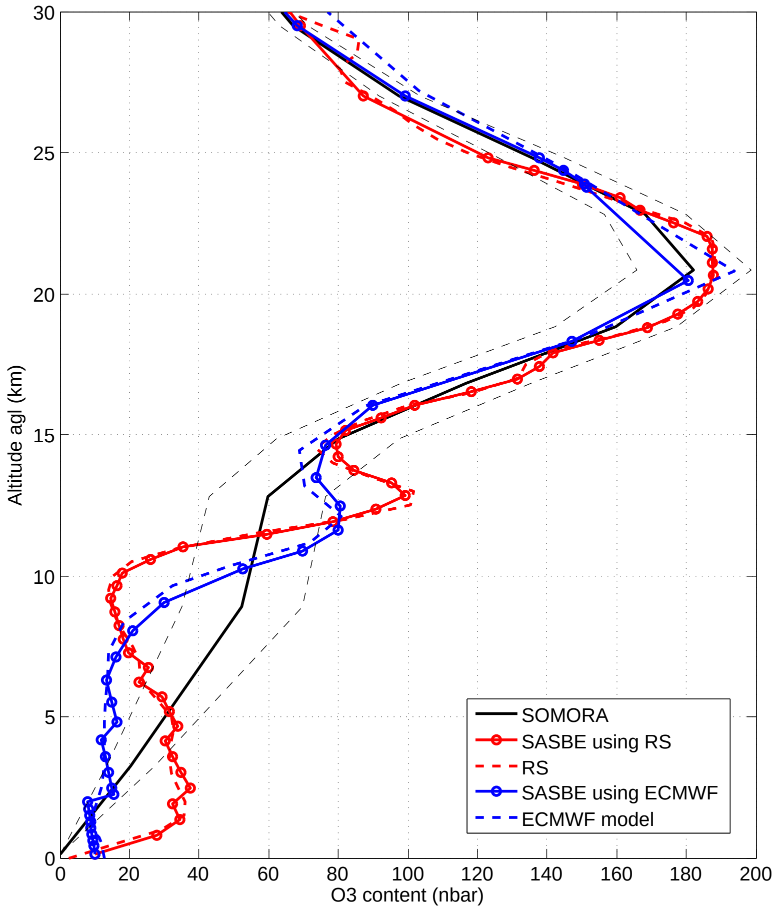

Figure 4. SOMORA ozone profile (in black), corresponding SASBE using RS ozone profile (in red), and SASBE using ECMWF model (in blue), RS ozone profile (in dashed red) and ECMWF simulated ozone profile (in dashed blue), Payerne, 24 January 2011, 12:00 UTC.

AMTD
8, 3399–3422, 2015

A method to derive the SASBE of ozone profiles

E. Maillard Barras et al.

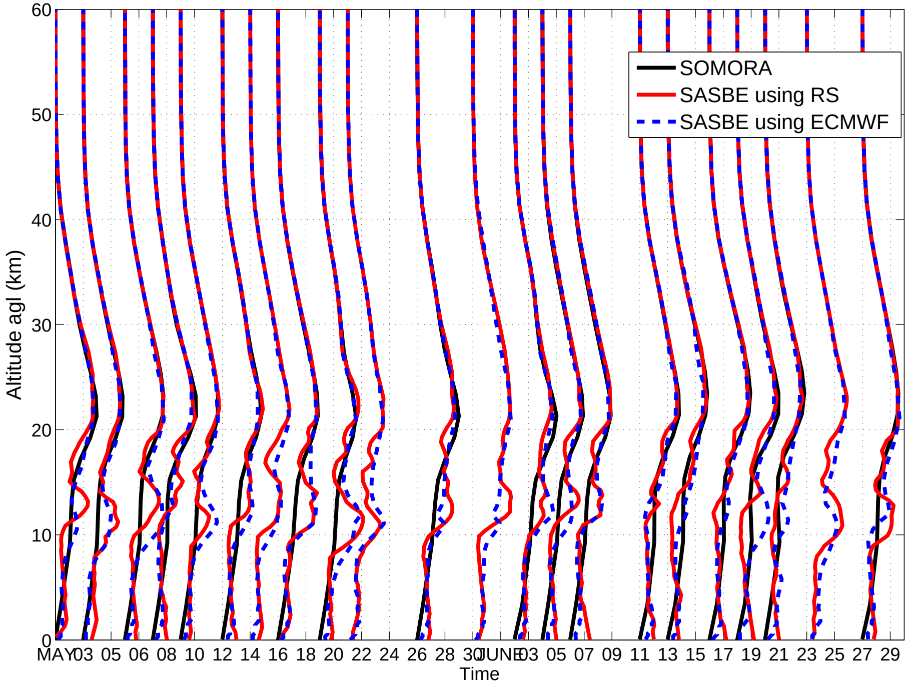

Figure 5. Time serie of ozone profile in nbar over Payerne for 2 months composed by MWR ozone profiles in the range of 20 to 65 km each 30 min (one per day plotted in black), SASBE ozone profiles 3 times a week (in red) in the range of ground up to 65 km and SASBE using ECMWF 4 times a day (one per day plotted in blue) in the range of ground up to 65 km.

AMTD
8, 3399–3422, 2015

A method to derive the SASBE of ozone profiles

E. Maillard Barras et al.

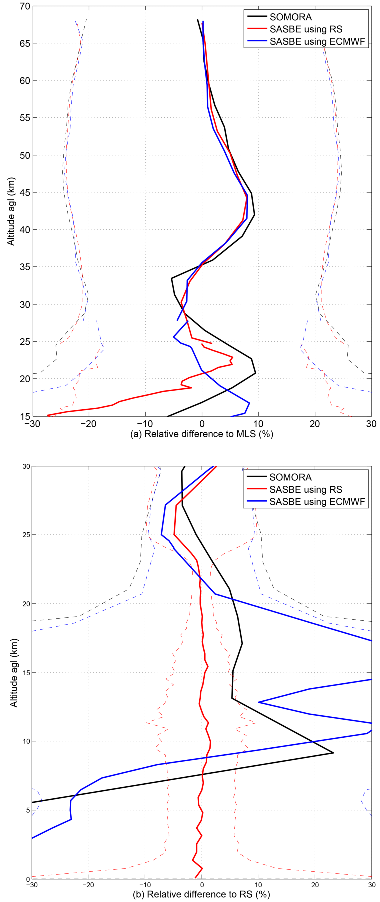

Figure 6. Ozone profile comparison of SOMORA in black, Payerne SASBE using RS in red and Payerne SASBE using ECMWF in blue with AURA/MLS **(a)** and Payerne radiosonde **(b)**. The ±1 SD of difference for SOMORA and for SASBE is plotted dashed.

AMTD
8, 3399–3422, 2015

A method to derive the SASBE of ozone profiles

E. Maillard Barras et al.